International Journal of Fatigue 32 (2010) 1928–1936

Contents lists available at ScienceDirect

International Journal of Fatigue

journal homepage: www.elsevier.com/locate/ijfatigue

Fatigue initiation behaviour throughout friction stir welded joints in AA2024-T3

H.J.K. Lemmen *, R.C. Alderliesten, R. Benedictus

Delft University of Technology, Faculty of Aerospace Engineering, PO Box 5058, 2600 GB Delft, The Netherlands

ARTICLE INFO

Article history:
Received 3 February 2010
Received in revised form 29 April 2010
Accepted 1 June 2010
Available online 9 June 2010

Keywords:
Friction stir welding
Fatigue initiation
Modified Goodman relation
Residual stress
Numerical analysis

ABSTRACT

This paper presents the results of an experimental and numerical investigation on the fatigue crack initiation behaviour of friction stir welded joints in AA2024-T3. These welds exhibit a complex material behaviour. In this study the influence of the different weld zones on the fatigue crack initiation behaviour was investigated. Therefore, fatigue experiments were conducted on a variety of welded central notched specimen configurations. As a result, the fatigue initiation life as function of the location in and the orientation of the weld was obtained. Numerical analyses were performed to investigate the influence of residual stress and yield strength on the stresses at the notch.

1. Introduction

Friction Stir (FS) welding attracts a growing interest as a high potential joining technology for aerospace applications [1,2]. Welding can offer a reduction in production costs and structural weight [3]. FS welding is a solid-state process, which makes it possible to join high strength aluminium alloys such as AA2024 and AA7075 [4]. The low process temperatures below solidus temperature assure a small heat impact with a good preservation of strength [5]. Furthermore, FS welding of aluminium alloys is a robust process without emission of hazardous gasses or radiation which requires protection.

To use FS welding in an airworthy structure, the fatigue behaviour and more specific Fatigue Initiation (FI) must be fully understood. Due to the often applied initial flaw approach, the reported research on FS welding in the literature, is mainly focussed on residual strength and Fatigue Crack Growth (FCG). In addition, most FI experiments are performed on commonly used dog-bone specimens (with K_t near 1), with the weld perpendicular to the applied load. These specimens will only result in the FI behaviour of the 'weakest' location in the weld, because there initiation will occur first. These dog-bone specimens do not include the effect of residual stresses, because the size is often too small for the residual stress to be maintained. By using centre notched FI specimens, the notch can be positioned at the location in the weld from which the FI life is desired. Moreover, a specimens width of 50 mm is large enough to maintain the residual stresses.

The objective of this research is to determine the FI behaviour at specific locations in FS welded AA2024-T3. Centre notch FI test specimens were used with notches of 1 mm in diameter. These notches were positioned at specific locations in the weld from which the FI behaviour is required. Furthermore, different orientations of the FS weld were investigated, to study how the orientation of the weld affects FI. To measure the FI life of each specimen, marker loads were applied which could be recognised at the fracture surface afterwards.

The residual stresses in the FS weld have been measured in a previous study [6]. A Finite Element (FE) analysis was performed to determine the influence of these residual stresses on the stresses at the notch in the FI specimens. These stresses obtained by FE analysis were used to predict the FI behaviour with the main stress effect approach.

2. Experimental

The purpose of this study was to investigate the influence of the different weld zones on the FI behaviour for different orientations of the weld. Therefore, specimens were manufactured with welds in two different orientations (Fig. 1), i.e. parallel to (*L–T* tests) and perpendicular to the applied load (*T–L* tests). Three test specimens were combined into one by placing three test sections above each other in a single specimen. Each test section contained an FS weld with a notch at a predefined location in this weld. By doing so, the duration of the test program was reduced significantly, because fatigue cycles could be applied to three notches simultaneously. The specimen had a width of 50 mm and the welds were placed 150 mm from each other to avoid influence from

* Corresponding author.
E-mail address: H.J.K.Lemmen@tudelft.nl (H.J.K. Lemmen).

0142-1123/$ - see front matter © 2010 Elsevier Ltd. All rights reserved.
doi:10.1016/j.ijfatigue.2010.06.001

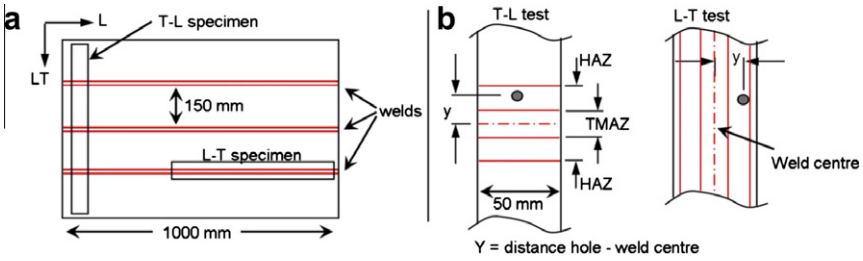

Fig. 1. (a) Example of how specimen are taken from the welded sheets and (b) details of how welds and holes are situated in the different test specimens.

one test section on the other. Once FI occurred in one test section, this section was cut off after failure and the test was continued on the remaining sections. Therefore, sheets were produced which contained three welds as is shown in Fig. 1.

2.1. Friction stir welding

The welds for this research were produced by EADS in Munich with an ESAB FS welding machine. For welding a tool with a featureless shoulder and a threaded triflute conical pin with a diameter of 13 and 5 mm, respectively, was used (Fig. 2a). All material welded for this research was obtained from the same sheet of AA2024-T3 with a thickness of 2.5 mm. Welding was performed parallel to the rolling direction with a tool tilt angle of $\alpha = 2°$ (Fig. 2a), a welding speed of 350 mm/min, a rotational speed of 550 rpm and a welding force of 19 kN. Prior to welding, the oxide layer was removed from the edge by a wire brush and the edge was cleaned with acetone. The sheets were clamped and a sheet of highly oxidized steel was placed below the specimens to prevent welding them to the table. Four sheets were welded together with a weld spacing of 150 mm for the *T–L* specimens (Fig. 1), whereas for the *L–T* specimens several sheets of 60 mm width and 600 mm long were welded together.

In general, three zones can be distinguished in the FS weld (Fig. 2b), the stirred zone or weld nugget, the Thermo-Mechanically Affected Zone (TMAZ), and the Heat Affected Zone (HAZ). All three zones have a different thermal and/or mechanical history, resulting in different microstructures and precipitation phases. Due to the rotation of the weld tool in combination with the traverse speed, the speed differences between the tool and the specimen is higher at one side than at the other side. These sides are defined as the Advancing Side (AS) and Retreating Side (RS) respectively (Fig. 2a).

2.2. Hardness tests

To determine the location and the size of the different zones in the weld, Vickers hardness tests were performed on cross sections of the welds along the centre line (Fig. 3). A load of 200 g was used for the hardness measurement. The spacing between each indentation was 0.2 mm. The hardness measurements were performed a few months after welding, giving the alloy time to naturally age.

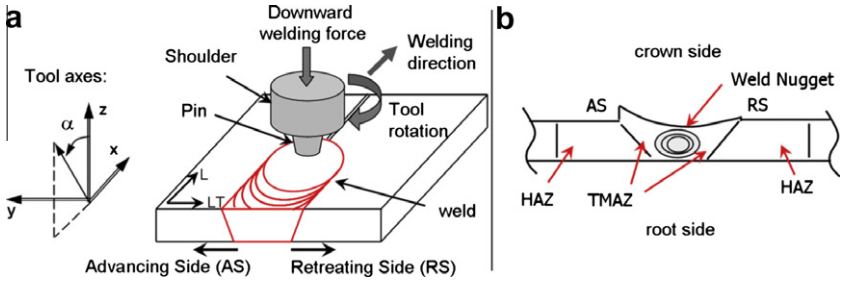

Fig. 2. (a) FS weld tool and definition of axes and (b) definition of weld zones.

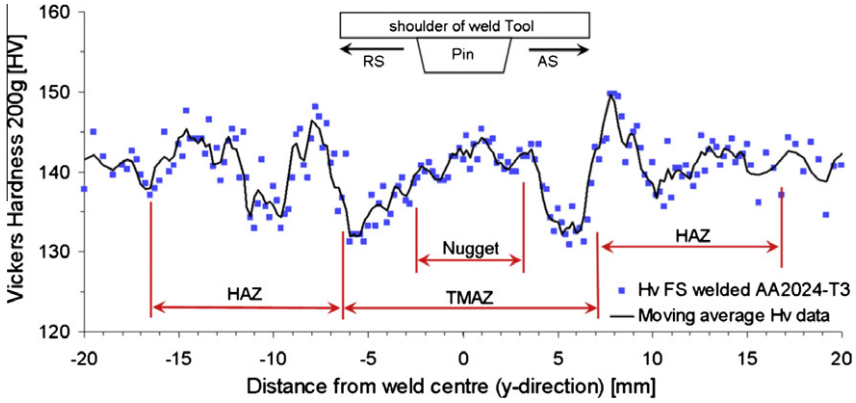

Fig. 3. Hardness profile from FS welded AA2024-T3.

The obtained hardness profile is typical for FS welded AA2024-T3 [5,7–9,4]. This profile was used to determine the locations of interest for the FI test specimens.

2.3. FI test specimen

To obtain the FI behaviour from a specific location in a single weld zone, a hole was drilled with a diameter of only 1 mm. Such a small notch is not common for centrally notched FI specimens, but the diameter had to be smaller than the size of the weld zone. As a result of the small notch diameter, an increased fatigue limit is expected due to the size effect [10]. However, for comparison this is not a problem because all tests were performed using specimens with equally sized holes, including the tests on the base material. For the *T–L* tests at least six specimens were produced and tested for each notch location, whereas for the *L–T* tests only four specimens were produced and tested per location.

Six locations were chosen based upon the hardness profile, i.e. $y = 0$ mm, 3 mm, 5.5 mm, 7.5 mm, 10.5 mm, and 12 mm (Fig. 3 and Table 1). Three of these locations coincide with local peaks and valleys in the hardness profile. Three other locations, including the centre of the weld, were chosen in-between these peaks and valleys to complete the set. Each location will be indicated in the text by its *y*-value which is the distance from the FS weld centre to the hole centre, according to the sign convention in Fig. 2a.

To produce the specimens, strips were cut from the welded sheets and machined to a width of 50 mm. The surface at the crown side was machined (0.1–0.2 mm) to remove the typical rough weld surface which affects FI. To remove the influence of machining and to create a well-defined surface, the crown surface was subsequently ground in two steps from P500 to P1000. The root side was not machined because no rough surface is present at this side of the weld. The small features which are present at the root side, like the centre line, were removed by the same grinding procedure as was applied on the crown side. The final thickness of the specimens was between 2.2 mm and 2.4 mm. Because the weld centre had to be visible to determine the location of the hole, grinding was performed after the holes were drilled and reamed. Aluminium tabs were adhesively bonded to the specimens' clamping areas, to prevent crack initiation there. The geometry of the *L–T* test specimens is asymmetric because the weld is at the centre of the specimen and the hole had to be drilled at one side of the weld. However, FE analysis showed no influence of this asymmetry on the stress at the notch.

Table 1
Location of the holes in the weld, with corresponding weld zone.

Location	0 mm	3 mm	5.5 mm	7.5 mm	10.5 mm	12 mm
Zone	Nugget	Nugget/ TMAZ	HAZ	HAZ	HAZ	HAZ

The same tests were performed on base material specimens to create a base line with which the result can be compared. these specimens exhibited the same geometry and production steps, except machining of the surface, as for the welded specimens. The material for these specimens was obtained from the same sheet as the material used for welding.

2.4. Fatigue experiment

The fatigue tests were performed using a MTS 100 kN servo hydraulic machine with an applied constant amplitude loading, a stress ratio of $R = 0.1$, and a frequency of 10 Hz. Each location in the weld was tested at a variety of stress amplitudes, ranging from 60 MPa to 100 MPa resulting in the *S–N* initiation curve (S–N_i) for that location. If specimens did not initiate before 10^6 cycles, the test was stopped and these data points were considered to be run-outs. After each 2500 baseline cycles, marker loads [11] were applied consisting of 5000 cycles with a stress ratio of $R = 0.7$, but with the same maximum stress. The maximum stress level was kept equal to avoid the influence of an overload on the fatigue life. The marker loads were performed with a frequency of 35 Hz. As a result of the marker loads, small bands in the fracture surface could be observed easily by optical microscopy. The bands were used to trace back the crack tip location and fatigue life of initiation (Fig. 4).

The fracture surfaces were harvested from the FI specimens after terminating the test. The distance between the marker load bands were measured by the aid of a stereo microscope (Fig. 4). Each marker load band was assigned to a certain fatigue life by correlating the visual measurements of the crack length during the test to the crack lengths measured at the fracture surfaces. The fatigue initiation life was backward calculated from these measurements.

The Potential Drop Method (PDM) was used to detect crack initiation. When a crack was detected with the PDM, the test was temporarily stopped until the crack length was measured using optical microscopes. Once initiated, the crack lengths were measured each 2500 cycles right before the marker loads were applied. Four crack lengths were monitored at each hole: at the left and right side of the hole and at the front and the rear side of the specimen.

Different definitions exist for the term Fatigue Initiation. In this study the definition of Schijve [10] is followed in which fatigue initiation is defined as the phase of the fatigue life including; cyclic slip, crack nucleation and micro crack growth. A crack length of 0.3 mm was chosen to be the FI crack length, because this length was short enough to exclude significant macroscopic fatigue fracture features and long enough to be determined sufficiently accurate in all specimens. As a consequence, this approach does not relate to the metallurgic definition of FI life, but is rather an engi-

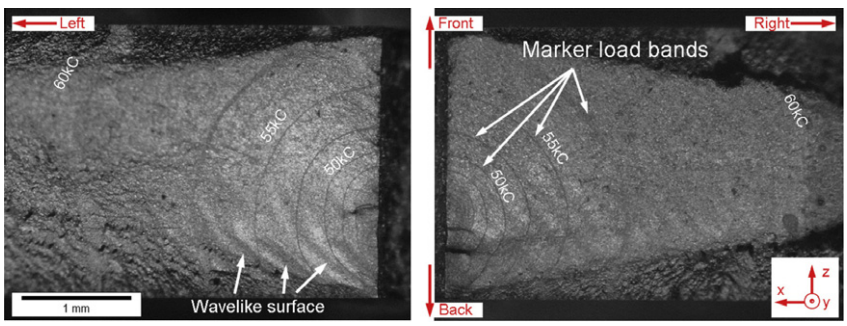

Fig. 4. Fracture surfaces from *T–L* tests, location: $y = 0$ mm, amplitude: 90 MPa.

neering approach; this crack length can be measured and the difference should be equal for all specimens tested at the same load.

2.5. Residual stress measurements

FS welding introduces residual stresses which are expected to have a significant effect on the FI life. To quantify the residual stress distribution, one of the FS welds used in this research has been subjected to residual stress measurements in a previous study using X-ray diffraction [6,12]. Residual stress measurements have been performed on several large specimens (40 cm by 20 cm) containing welds in as-welded condition and on a FI *L–T* test specimen prior to testing. The latter specimen received the same surface treatment as is described previously. Fig. 5 presents the measured residual stress profiles obtained from both specimens.

The residual stresses are highly orientation dependent, because the longitudinal stresses (parallel to the weld) are 100–175 MPa, whereas the axial stresses (perpendicular to the weld) are negligible. Therefore, different response is expected from the *L–T* and *T–L* FI specimens. Differences are also observed between the longitudinal stress profiles from the crown and root side; at the root side two peaks exist at 7 mm from the weld centre, whereas the crown side exhibits a more flat profile in the centre region. Fig. 5 shows that the residual stresses are lower in the FI specimen than in the original as-welded condition. This stress relaxation occurred when the specimen was machined to a width of 50 mm.

2.6. Finite element analysis

A 3D FE analysis was performed to obtain the stress level at the notch in the welded FI *L–T* specimens. The weld is represented in the FE model by the residual stress profile and the yield strength profile, which both have been measured in a previous study [6,12]. The details of this FE analysis will be published in the future, but that paper was not finished at the moment that this work was submitted.

Two different load cases were applied in the FE analysis for each hole location; the maximum and minimum stress level of the fatigue cycle. From each load case the peak stress at the notch was obtained with which the mean stress and stress amplitude at the notch were calculated. The mean stress at the hole vary through the thickness of the specimen, therefore, only the maximum value is used in this study because FI occurs at the location along the notch with highest mean stress. The FE analysis on each hole loca-

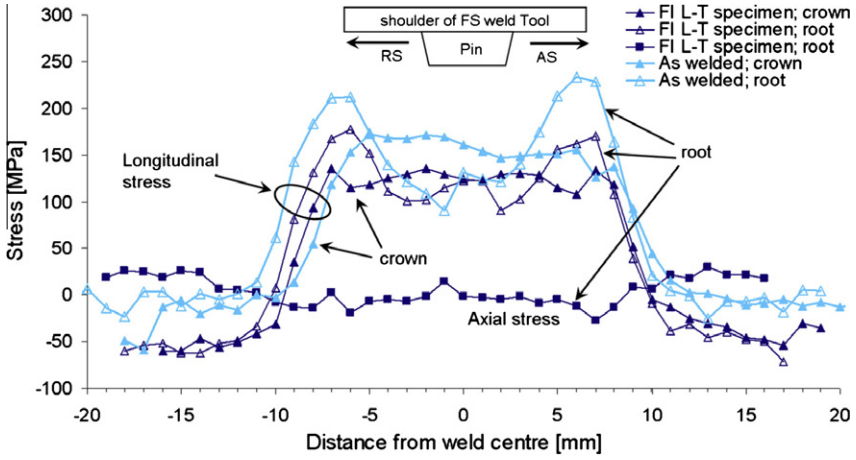

Fig. 5. Residual stress profile from FS welded AA2024-T3 [6].

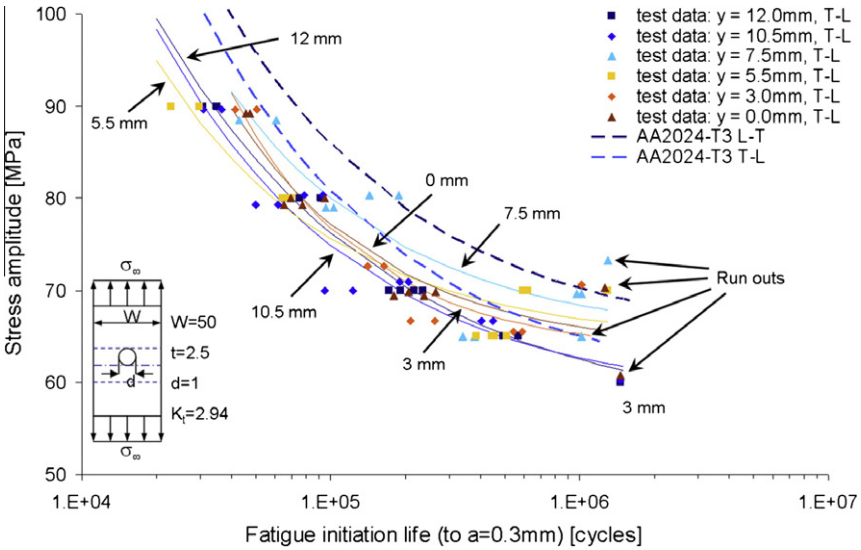

Fig. 6. Results from the *T–L* FI tests, i.e. FI life's and $S–N_i$ curves from the locations at the advancing side of the FS weld together with base material $S–N_i$ curves.

tion was performed for the same fatigue loads as was applied in the experiments to obtain the S–N_i curve.

To validate the results, the FE analysis is also performed on two base material specimens with hole locations of $y = 0$ mm and 7.5 mm without residual stresses. These two analysis provide the fatigue stresses at the notch for the base material FI tests which are correlated to the results of the FE analysis on welded FI specimens. Moreover, the difference between the results from these two FE analyses is a measure for the influence of the asymmetric geometry in the centre notch FI specimen.

3. Results

3.1. Fatigue initiation test results

The fatigue initiation test results are presented in Figs. 6 and 7. A four parameter Weibull S–N_i curve is fitted through the data points. Note that due to curve fitting each data point is considered as of equal weight, which may be considered inadequate for the run-outs. Therefore, the trend lines have to be treated with some care in the high cycle region above 800 kc.

The FI results from the T–L tests are presented in Fig. 6 together with the base material T–L and L–T test results. In general, the S–N_i curves of the FS welded material are below the S–N_i curve of the base material. However, no significant differences are observed between the S–N_i curves obtained for different locations in the weld. All data is located within the same scatter band.

Fig. 7 displays the L–T test results together with the base material S–N_i curves. In contrast to the T–L test results, the L–T data show significant differences between the FI lives obtained at different locations in the FS weld. The differences are not only observed in the low cycle fatigue regime, but also near the fatigue limit. The results from location $y = 12$ mm exhibits the best FI behaviour, even better than the base material. The results from location $y = 10.5$ mm exhibits results similar to the base material, but the slope of the S–N_i curve is different. All the other locations exhibit FI lives significantly shorter than the base material. Although the slopes of the S–N_i curves are different for each location, some care must be taken when drawing conclusions from this observation, because the S–N_i curves are mostly based upon a small amount of data points. From all the S–N_i curves, the results from $y = 0$ mm show the worst FI behaviour below 100 kc, whereas $y = 7.5$ mm exhibits the worst FI behaviour beyond 100 kc.

3.2. Results from the FE analysis

The FE analysis has been verified successfully with a mesh dependency analysis and validated with the results from the base material. FE analysis was also used to verify whether the asymmetric position of the notch in the L–T test specimens had an influence on the stress levels at the notch. The FE analysis on a base material specimen with the notch at 7.5 mm from the specimens centre showed no difference between the stresses from both sides of the notch and from the specimen with a notch at the centre line. Therefore, it is assumed that the asymmetric notch position has no influence on the welded L–T tests specimens either.

The FE analysis showed significant impact of plasticity on the maximum stresses at the notch. The theoretical linear-elastic stress levels at the notch are fairly high because of the stress concentration factor of $K_t = 2.94$. However, the stress at the notch was reduced as soon as the yield stress was reached because plasticity acts as a damping effect on the stress concentration factor. The consequence of this damping effect is an inverse relation between the applied nominal stress amplitude and the mean stress at the notch. This inverse relation is shown in Fig. 8, where the mean stress at the notch is plotted as a function of the applied stress amplitude for the base material. Initially for low stress amplitudes the mean stress response at the notch is only a function of the Young's modulus and the stress concentration factor (linear-elastic response), but beyond the yield point, the response of the mean stress becomes highly non-linear. The yield point indicated in the figure is defined as the point at which the stress–strain curve deviates from the linear part and not as the material definition of 0.2% yield strength.

Fig. 9 presents the mean stress response from the FE analyses on welded specimens. The mean stress response is plotted for each notch location and for both sides of the notch together with the base material mean stress response as was plotted in Fig. 8. The differences between the curves from welded specimens and the base material curve is a direct effect of the residual stress profile in the weld. A mean stress above the base material curve is observed for the locations, where the residual stress profile exhibits

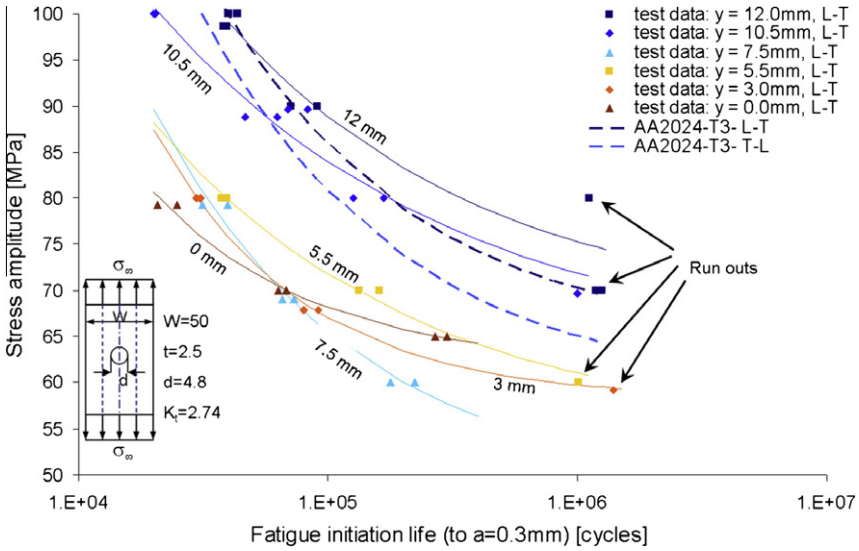

Fig. 7. Results from the L–T FI tests, i.e. FI life's and S–N_i curves from the locations at the advancing side of the FS weld together with base material S–N_i curves.

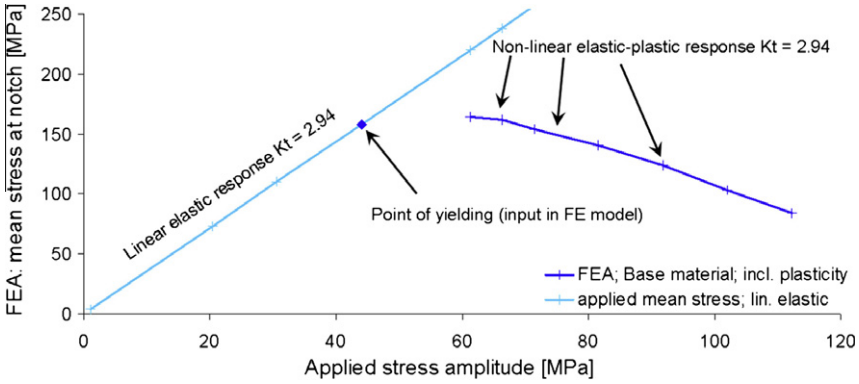

Fig. 8. FE analyses: response of the mean stress at the notch due to the applied stress amplitude on base material specimens.

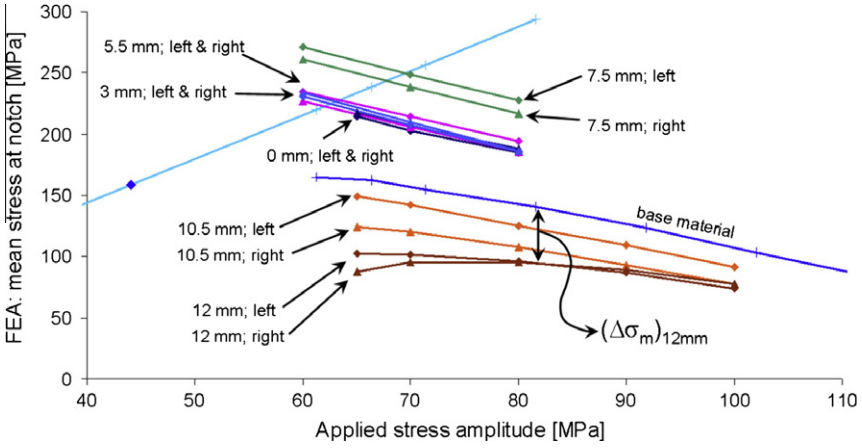

Fig. 9. FE analyses; mean stress levels as function of the applied stress amplitude for each hole location in the welded specimens; curves are plotted for both the left and right side of the hole.

tensile stress (y = 0 mm, 3 mm, 5.5 mm, and 7.5 mm), whereas a mean stress below the base material curve is observed for the locations, where the residual stress profile exhibits compressive stress (y = 10.5 mm and 12 mm). The difference between the mean stress in the welded specimens and the base material specimens is indicated by delta mean stress (ΔS_m).

The coherence of the delta mean stress with the residual stress varies for different applied stress amplitudes (Fig. 9). The reason for this non-linear behaviour is the non-linear plastic behaviour of the material and the different yield strength in the FS weld. If the hole is situated in a region with low yield strength the maximum stress at the notch will be lower than for a hole in a region with high yield strength. Moreover, a location with high residual stress will reach the yield point at a lower applied stress, and thus exhibits more plasticity than a location with low residual stress.

Unlike the mean stress, which is dependent on the maximum and minimum stress, and thus limited by local material properties, the stress amplitude is not affected and is only dependent on the stress concentration factor K_t as is illustrated by Eq. (1). Therefore the change in fatigue load due to residual stresses can be described by the mean stress effect only.

$$S_{a(Notch)} = S_{a(FEA)} = K_t \cdot S_{a(Applied)} \quad (1)$$

3.3. Prediction model

Because the residual stress only affects the mean stress, it is possible to use the mean stress effect to predict the FI behaviour in the FS weld using the base material FI behaviour. This prediction method requires two data sets: the fatigue diagram of the base material AA2024-T3, and the delta mean stress at the location of interest. The fatigue diagram is reconstructed from the S–N_i curve of the base material (presented in Figs. 6 and 7), using the modified Goodman relation (Eq. (2)) [13–15].[1]

The mean stress at the notch (obtained from the FE analysis) is used for the prediction instead of the applied mean stress. Consequently the mean stress of the notch is also used in the modified Goodman relation. The relation between the stress amplitude at the notch and the applied stress is already described by Eq. (1). The analytical stress concentration K_t = 2.94 is slightly different from what was obtained from the FE analysis; K_t = 3.1. It was decided to use the stress concentration factor obtained by the FE analysis. Furthermore, a relation between the mean stress (Sm) at the hole, and the applied stress amplitude ($S_{a(Applied)}$) was obtained by fitting a four degree polynomial through the data of the base material in Fig. 8.

The relation between the FI life and the stress amplitude at the notch is described by a fitted Weibull curve as was used previously to obtain the curves in Figs. 6 and 7. This Weibull curve is used to create the fatigue diagram based upon the modified Goodman relation (Eq. (2)). As can be seen from the modified Goodman relation, each line in the fatigue diagram is described by two constants, the ultimate strength (S_{ult}) and the stress amplitude for a zero mean

[1] Goodman never published his theory as such (p. 297 [14]), only in an exercise book for mechanics [13] he refers to Gough [15] who mentions the modified Goodman relation.

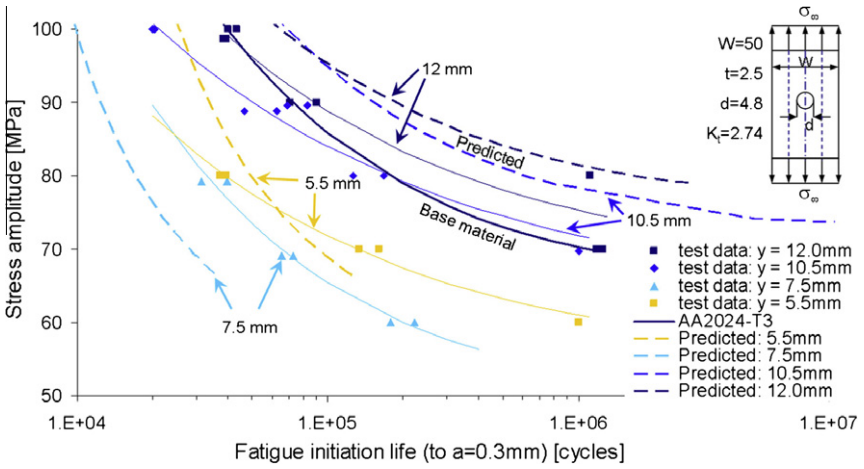

Fig. 10. Predictions of FI S–N_i curves together with test data.

stress ($Sa_{(Sm=0)}$). The ultimate strength is equal for each constant life curve in the fatigue diagram, whereas the latter ($Sa_{(Sm=0)}$) is obtained by substituting the Sa and Sm for each FI life (Weibull curve) into the modified Goodman relation.

$$\frac{Sa_N}{(Sa_N)_{Sm=0}} + \frac{Sm_N}{S_{ult}} - 1 = 0 \tag{2}$$

Because each curve is described by $Sa_{(Sm=0)}$, a relation exists between this constant and the FI life. A function was fitted which described this relation best (Eq. (3)). In this function; a–d are fit constants and N is the fatigue life (in this case: $a = 561.77$, $b = 217.32$, $c = 276.64$, and $d = 0.56095$).

$$N = \left\{ \frac{b \cdot (Sa)_{Sm=0} - a \cdot b}{c - (Sa)_{Sm=0}} \right\}^{1/d} \tag{3}$$

To predict the fatigue lives for the mean stresses obtained by FE analysis on welded specimens (Fig. 9), the mean stress for a certain location and the corresponding stress amplitude are substituted into Eq. (2). As a result $Sa_{(Sm=0)}$ is calculated from which the corresponding fatigue life is found using Eq. (3). By following this approach for all data points in Fig. 9, it is possible to predict the S–N_i curves for the different locations in the weld. Instead of calculating the fatigue life for the individual data points, the delta mean stress (ΔSm) was applied on the S–N_i curve of the base material. The delta mean stress if represented by a linear function of the stress amplitude because the delta mean stress is not constant for different stress amplitudes (Fig. 9). As a result of the varying delta mean stress, the S–N_i curve of the base material is not only translated, but also rotated for different locations in the weld.

Fig. 10 presents the predictions for four locations, i.e. $y = 5.5$ mm, 7.5 mm, 10.5 mm, and 12 mm. All four predicted curves show the trend which is theoretically expected; a decrease of the fatigue life and the fatigue limit for tensile residual stresses and an increase of the fatigue life and the fatigue limit for compressive stresses. The shape of the S–N_i curves are also changed because the delta mean stress is not constant for all stress amplitudes. The accuracy of the prediction can be evaluated using two observations: the magnitude of the shift of the S–N_i curve and the gradient of the S–N_i curve compared to the test data.

4. Discussion

4.1. Fatigue initiation test results

The influence of the residual stress profile (Fig. 5) is recognised in the FI behaviour of the L–T specimens (Fig. 7). At $y = 12$ mm, compressive residual stresses provide the longest FI life. At $y = 10.5$ mm the residual stress field is slightly below 0 MPa and thus the FI life is equal to the base material. The S–N_i curves for the locations $y = 0$ mm, 3 mm, 5.5 mm, and 7.5 mm are all shifted down and to the left, which corresponds to the tensile residual stress in this region. Because $y = 7.5$ mm is located at the peak in the residual stress profile, it was expected to find the lowest FI lives at this location. This is indeed the case above 100 kc, but for lower fatigue lives location $y = 0$ mm exhibits the lowest fatigue behaviour.

The results of the T–L specimens presented in Fig. 6, show no significant difference between the different locations. Only a small difference with the base material test results is observed, because all locations in the FS weld exhibit lower FI life. This is attributed to microstructural changes in the material as a result of welding.

Based upon the experimental data, it is concluded that the residual stresses have a significant larger influence on FI (Fig. 7) than the welding induced microstructures (Fig. 6).

4.2. Contribution of FE analysis and the prediction method

The FE analysis has been performed to understand how residual stresses in the FS weld affect the stresses at the different notch locations. The FS weld is represented in the FE analyses by the residual stress profile and the yield strength profile. Unfortunately, still some assumptions were necessary, like the through thickness mechanical behaviour in the weld. Therefore, the results of the FE analysis are useful for comparison reasons, but should always be treated with some care. Nonetheless, the FE analysis is the only method to obtain the stress state at the notch in a FI test specimen with a FS weld.

The most important results from the FE analysis are presented in Fig. 9; the mean stress at the notch as function of the applied stress amplitude for each hole location. Comparison with Fig. 7 shows a correlation between the magnitude of mean stress and the FI lives. The rise or fall of the S–N_i curves corresponds with the rise or fall of the mean stress due to the residual stress at that location. This relation is confirmed by the analytical prediction method for the FI behaviour as is presented in this study (Fig. 10). Two parameters are used to qualify the prediction method; the absolute difference between the test results and the predicted S–N_i curve, and the difference in gradient between these two.

The predicted S–N_i curves are over-predicted for all locations except for $y = 5.5$ mm. A reason for this over-prediction can be the use of the improved Goodman relation which is a simplification

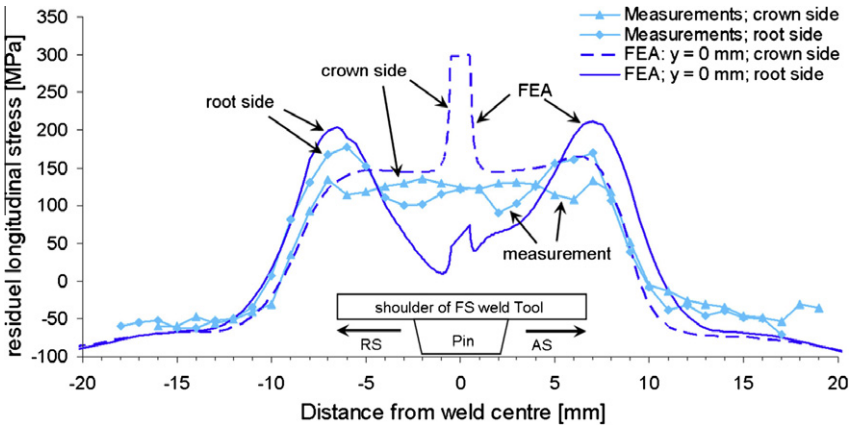

Fig. 11. Comparison of residual stress profile within FE model and measured residual stress profile.

of the fatigue diagram [10]. A small change in the angle of the curves in the fatigue diagram leads to a significant increase or decrease of the mean stress effect. Moreover, the mean stress effect has been validated in the past for small changes in mean stress, whereas, the delta mean stresses are relatively large in these predictions (Fig. 9). The error introduced by using the improved Goodman relation will only increase for larger delta mean stresses. It is expected that the prediction is improved if a more realistic representation for the fatigue diagram is used. Unfortunately, no fatigue diagram is available in the handbooks for the specimen geometry used in this study (notch diameter of 1 mm) [16]. It is possible to obtain the fatigue curve for the proper stress concentration factor K_t, but these curves neglect the size effect which is significant for the used notch diameter.

After examination of the measured residual stress profile in the FI specimens and the residual stress profile in the FE model, a difference has been observed that explains a portion of the over-prediction. For the FE analysis the residual stress profile from a large sheet with a weld in as-welded condition was used. This residual stress profile was introduced in the geometry of the FI specimen which results in redistribution of the stresses due to the small width of the specimen. It was assumed that this redistribution would lead to the residual stress state as was present in the real *L–T* FI specimens. However, as can be seen in Fig. 11, the residual stress profile in the FE analysis are different for the measured residual stress profile in the FI specimen. At the locations $y = 5.5$ mm and 7.5 mm the residual stresses in the FE model are larger, whereas at $y = 10.5$ mm and 12 mm the residual stresses are lower than the measured residual stresses. Both differences result in a larger delta mean stress and thus an over-prediction of the FI life.

The mismatch in the gradient between the predictions and the test data in Fig. 10 is for some locations in the weld significant. At this moment, it is not understood what the reason is for this behaviour. Significant differences are observed for the gradients in the test results (Fig. 7). The predictions do not copy this behaviour, therefore, these changes in gradient in the weld is attributed to other mechanisms then the residual stress or the yield strength. It might be that the fine grained microstructure with low angle grain boundaries in the nugget plays an important role for the FI behaviour. It was expected that the influence of the microstructure was small because a small decrease of FI life was observed for the *T–L* test results (Fig. 6). The FI behaviour in these tests was not affected by the residual stress, only the microstructure. However, these tests are not conclusive for the FI behaviour in the *L–T* specimens, because the microstructure in the nugget and the TMAZ is highly anisotropic. Therefore, the effect of the microstructure on the FI behaviour can be anisotropic too.

From previous observations it can be concluded that a correlation exists between the mean stress obtained by FE analysis and the FI behaviour obtained by testing. The differences observed between the *T–L* tests and the *L–T* tests can be attributed to the residual stresses in the FS weld.

5. Conclusions

The fatigue initiation properties depend on the orientation of the FS weld. Furthermore, when the FS weld is parallel to the applied load, the FI behaviour is also dependent on the location in the weld. This dependency is caused by the presence of residual stresses, which are negligible perpendicular to the weld (*T–L*), but significant parallel to the weld (*L–T*).

The microstructure in the FS weld has an influence on the FI behaviour, but this effect is smaller than the influence of residual stresses.

A successful detailed FE analysis is performed to understand the influence of the residual stresses in the FS weld on the FI behaviour better. These FE analysis results have been used to predict FI in the weld. It is shown with this prediction that the differences observed between the *L–T* and *T–L* FI test results can be attributed to the residual stresses in the weld.

Although FE analysis is a powerful tool, it must always be treated with some care. Some assumptions had to be made to model the FS weld by a residual stress field and a yield strength profile. Therefore, the quantitative results will be different in details from the reality.

Prediction of the FI behaviour in the FS weld is possible by using the mean stress effect. However, a more realistic representation of the fatigue diagram is required. The modified Goodman relation has been used in this work, but for large changes of mean stress this representation of the fatigue diagram introduces significant errors.

Acknowledgments

The authors wish to thank Dr. J. Silvanus from EADS Innovation works Germany, Metallic technologies and Surface engineering, for the ability to use the friction stir weld machine to produce the specimen. Mr. E.R. Peekstok from the Delft University of Technology, department: Microstructural Control in Metals, for his help

by the preparation of the microscopy samples and the use of the microscopes.

References

[1] Dunkerton SB, Vlattas C. Joining of aerospace materials – an overview. Int J Mater Prod Technol 1998;13(1–2):105–21.
[2] Bolser D, Talwar R, Lederich R. Mechanical and corrosion properties of friction stir welded 7050–t7451 aluminium alloy. Weld World 2005;49(3/4):27–33.
[3] Pacchione M, Werner S, Ohrloff N. Design principles for damage tolerant butt welded joints for application in the pressurized fuselage. Napels: ICAF; 2007.
[4] Mishra R, Ma Z. Friction stir welding and processing. Mater Sci Eng 2005;50:1–78.
[5] Biallas G, Donne CD, Juricic C. Monotonic and cyclic strength of friction stir welded aluminium joints. Adv Mech Behav Plast Damage 2000;1:115–20.
[6] Lemmen H, Alderliesten R, Benedictus R, Pineault J. Local yield strength and residual stress measurements on friction stir welded aa2024-t3, aa7075-t6, and aa6013-t4. J Aircra, 2010, accepted for publication.
[7] Booth DPP, Starink MJ, Sinclair I. Analysis of local microstructure and hardness of 13 mm gauge 2024-t351 aa friction stir welds. Mater Sci Technol 2007;23(3):276–84.
[8] Jones M, Heurtier P, Desrayaud C, Montheillet F, Allehaux D, Driver J. Correlation between microstructure and microhardness in a friction stir welded 2024 aluminium alloy. Scripta Mater 2004;52:693–7.
[9] Jata K. Friction stir welding of high strength aluminium alloys. Mater Sci Forum 2000;331–337:1701–12.
[10] Schijve J. Fatigue of structures and materials. Delft: Kluwer Academic Publishers; 2001.
[11] Schijve J. Application of marker load systems for fractography of fatigue cracks, a proposal for experiments. Technical report. Delft University of Technology, Faculty of Aerospace Engineering, Structures and Materials Laboratory; 2001.
[12] Lemmen HJK, Alderliesten RC, Pieters RRGM, Benedictus R, Pineault J. Influence of local yield strength and residual stress on fatigue in friction stir welding. In: 49th AIAA/ASME/ASCE/AHS/ASC structures, structures dynamics, and materials conference, AIAA, Schaumburg, IL; 2008, p. 22.
[13] Goodman J. Mechanics applied to engineering. Longmans, 9th ed., vol. 1. London: Green and Co. Ltd; 1926.
[14] Budynas-Nisbett, Mechanical engineering. Shigley's mechanical engineering design, 8th ed., McGraw-Hill Primis.
[15] Gough J. The fatigue of metals. London: Scott Greenwood; 1926.
[16] Handbuch Struktur Berechnung (HSB), German aeronautical handbook under responsibility of the German Industrie Ausschuss Struktur Berechnung (IASB) part of German Luftfahrttechnisches Handbuch LTH; 1994.